A Hypoelastic Model of Soils Accounting for Failure

Un Modèle Hypoélastique des Sols Comportant la Rupture

D.BATTELINO and
B.MAJES Department of Civil Engineering, University of Ljubljana, Yugoslavia

SYNOPSIS In this paper the soil has been treated as a "hybrid hypoelastic body". The stress-strain relationships as observed in triaxial testing have been presented by two families of charts relating tangent values of compression and shear moduli to octahedral stresses. For the use in the finite element analysis of settlements and plastification of soils such charts have been expressed by sets of coordinate values and the interpolation was made by applying spline functions. The procedure has been proved successful provided that the stress paths to which the triaxial specimens had been subjected, are similar to those which have to be expected in the soil layer.

INTRODUCTION

The hypoelastic constitutive law for soils which Kulhawy, Duncan and Sied (1969) had based on Kondner's hyperbolic stress-strain relationship proved useful in forecasting displacements of soils below dams and foundations. The shortcoming of simple hypoelastic models is their dependence on stress history and actual stress path. The elastic-plastic models are able to express the deformability of soils in a more general way and recently important progress has been made in developing them (see e.g. Lade and Duncan 1975, Prévost and Höeg 1975). On the other hand, Darve (1974) succeeded in forming a generally valuable hypoelastic model as well. Now, the determination of a great number of physical parameters determining the constitutive laws in their generalized form requires very extensive experimental work, and there is not enough experimental evidence available for separating cases and conditions when general models can be used in a simplified form. Thus, the direct interpretation of experimental data seems to be still of interest for practical aplications provided that the stress paths of experiments approach the stress paths appearing in the problem in question.

In the present paper, the measurements made on cylindrical samples in triaxial compression tests have been expressed in terms of octahedral values of stresses and strains. For the use in computing settlements by the finite element method, families of compression and shear tangent moduli have been deduced. Since all stress states up to the failure are included, the development of stresses and strains in soil bodies up to the failure could be persued. The seepage resistance has been considered in an approximate way. Viscous soil properties were not taken into account.

TANGENT MODULI IN TERMS OF OCTAHEDRAL STRESSES

If in drained triaxial tests on cylindrical samples with slowly increasing stress levels axial (ε_1) and volume strains (ε_v) have been measured, the results can be expressed in terms of octahedral values of strains ($\varepsilon_{oct} \equiv \varepsilon^0$, $\gamma_{oct} \equiv \gamma^0$) and effective stresses ($\sigma'_{oct} \equiv \sigma^{0\prime}$, $\tau_{oct} \equiv \tau^0$).

$$\varepsilon^0 = \left[\varepsilon^0(\sigma^{0\prime})\right]_{\tau^0=\text{const}}, \quad \gamma^0 = \left[\gamma^0(\tau^0)\right]_{\sigma^{0\prime}=\text{const}} \quad (1),(2)$$

whereby

$$\varepsilon^0 = \varepsilon_v/3, \quad \gamma^0 = (3\varepsilon_1 - \varepsilon_v)\sqrt{2}/3 \quad (3),(4)$$

$$\sigma^{0\prime} = (\sigma_1 + 2\sigma_3)/3, \quad \tau^0 = (\sigma_1 - \sigma_3)\sqrt{2}/3 \quad (5),(6)$$

For the use in numerical computations the families of charts (1) and (2) can be given analytical expressions or, more generally, they can be presented by sets of point values and interpolation may be made by using spline functions (Desai 1971).

In the relationship (1) the role of the shear stress is not very important and in several cases it can be neglected. Thus, the family of charts (1) can then be replaced by a single line: $\varepsilon^0 = \varepsilon^0(\sigma^{0\prime})$ (1-a). The charts, however, relating shear strains to shear stresses are strongly affected by spheric stress $\sigma^{0\prime}$ (Eq.2). The analytical presentation of the whole set of charts is not possible except in an approximate way or in a somewhat limited stress domain. If one wants to express the trend of deviatoric strains to increase towards infinity when approaching the failure, the numerical presentation of test data is preferable.

When analyzing the stress and strain states in soil bodies by the finite element method, the relationships (1), (1-a resp.), and (2) have to be linearized in single small loading steps. Tangent values of compression (K) and

shear (G) moduli may be deduced according to their definition by:

$$K=\frac{1}{3}\frac{\partial\sigma^{0\prime}}{\partial\varepsilon^{0}}\quad,\quad G=\frac{\partial\tau^{0}}{\partial\gamma^{0}} \qquad (7),(8)$$

Now, if choosing the numerical presentation of charts (1) and (2), the differentiation (7) and (8) by using splines has been found very sensitive to small inaccuracies in numerical data. For this reason it is preferable first to deduce the moduli for the whole stress domain, to present the results graphically and draw the best continuous fitting lines:

$K=\left[K(\sigma^{0\prime})\right]_{\tau^{0}=\text{const}}$ (9) or $K=K(\sigma^{0\prime})$ (9-a)

$$G=\left[G(\tau^{0})\right]_{\sigma^{0\prime}=\text{const}} \qquad (10)$$

The above sets of lines may now be expressed by sets of point values; the moduli which correspond to the stress states appearing in single finite elements at successive loading steps, can then be interpolated by using spline functions.

EXAMPLES OF EXPERIMENTAL RESULTS

The following two examples of the charts (9-a) and (10) refer to triaxial compression tests of which each is made on a single specimen; the stress paths which were applied are shown in the figures. Owing partly to anisotropic effects causing deviatoric displacements at hydrostatic stress states, and partly to plastic deviatoric strains remaining after the decrease of the stress level, positive γ^{0} values appeared at $\tau^{0}=0$ in the original charts $\gamma^{0}=\left[\gamma^{0}(\tau^{0})\right]_{\sigma^{0\prime}=\text{const}}$. In Figs. 2a and 4a all charts have been moved along the γ^{0} axis into the origin of the coordinate system (τ^{0},γ^{0}). This displacement does not affect the values of tangent shear moduli if expressed in terms of octahedral stresses.

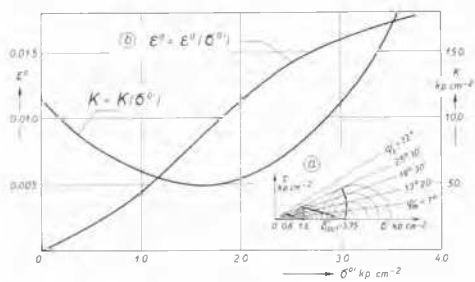

Fig.1 A silty sand: (a)stress-path; (b)spheric strain (ε^{0}) and compression modulus (K) versus effective spheric stress ($\sigma^{0\prime}$) diagrams.

Figs. 1 and 2 present the deformability of a silty sand whose strength is $\tau_{f}=\tan 32^{0}\sigma'$, while Figs. 3 and 4 are related to a very compressible silty clay of the Ljubljana Marsh with the inclination of the failure envelope of Mohr's stress circles $\phi'=24^{0}$. In the $\varepsilon^{0}=\varepsilon^{0}(\sigma^{0\prime})$ diagram of Fig.1 points represent values obtained for different stress states, proving little effect of shear stresses on the $\varepsilon^{0}=\varepsilon^{0}(\sigma^{0\prime})$ relationship. A somewhat greater deviation of $\varepsilon^{0}=\left[\varepsilon^{0}(\sigma^{0\prime})\right]_{\tau^{0}=\text{const}}$ charts for the clayey specimen from the chosen representative line

$$\left[\varepsilon^{0}\right]_{\tau^{0}/\sigma^{0\prime}=0.2\,0.6}=a+b\,\ln(c+d\sigma^{0\prime}) \qquad (11)$$

(numerical values of parameters a, b, c, d are given in the figure) is indicated in Fig. 3-b by the narrow zone between the charts

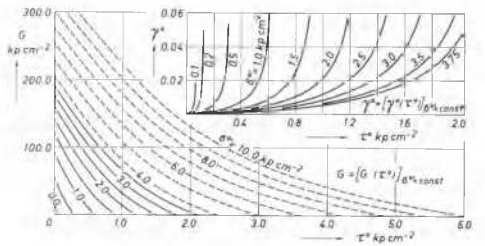

Fig.2 A silty sand: (a)$\gamma^{0}=\left[\gamma^{0}(\tau^{0})\right]_{\sigma^{0\prime}=\text{const}}$, (b)$G=\left[G(\tau^{0})\right]_{\sigma^{0\prime}=\text{const}}$; dashed lines have been obtained by way of extrapolation.

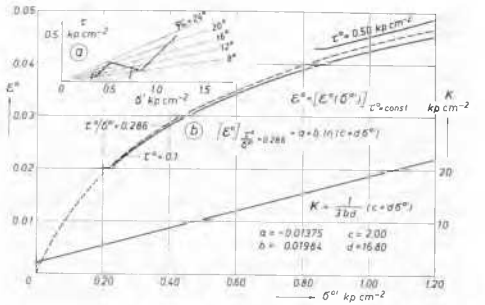

Fig.3 A marsh clay: (a)stress-path, (b)spheric strain (ε^{0}) and compression modulus (K) versus effective spheric strain ($\sigma^{0\prime}$) diagrams.

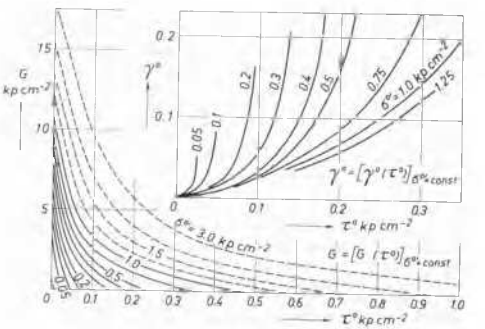

Fig.4 A marsh clay: (a)$\gamma^{0}=\left[\gamma^{0}(\tau^{0})\right]_{\sigma^{0\prime}=\text{const}}$, (b)$G=\left[G(\tau^{0})\right]_{\sigma^{0\prime}=\text{const}}$; dashed lines have been obtained by way of extrapolation.

corresponding to τ^0=0.1 and 0.5 kp cm^{-2}. The differentation of Eq. (11) has given the analytical expression for the K versus $\sigma^{0\prime}$ relationship in the form

$$K=(c+d\sigma^{0\prime})/3bd \qquad (12)$$

Points appearing in the diagram $\gamma^0=\gamma^0(\tau^0,\sigma^{0\prime})$ of Fig. 4-a represent values obtained by the numerical integration of the $G=G(\tau^0,\sigma^{0\prime})$ charts presented in Fig. 4-b. They prove the satisfactory accuracy of the procedure explained in the preceding section.

APPLICATION OF TANGENT MODULI IN COMPUTING STRESSES AND DISPLACEMENTS

A computer program was prepared for the computation of stresses, strains and displacements for plane-strain or plane-stress problems by using the finite element method (see also Saje 1974, Majes 1974). In every load interval the deformability of single elements is represented by tangent values of the deformation modulus (E_t) and Poisson's ratio (ν) corresponding to the compression (K) and shear (G) moduli as obtained by the procedure explained in the preceding sections. Similar results from plane-strain triaxial tests may preferably be used. As they were not at our disposal, the results obtained on cylindrical samples were applied in the following example.

A layer (h = 6.75 m) consisting of the marsh clay whose deformability has been presented in Figs. 3 and 4, is subjected to a vertical surface load-strip of trapezoidal cross-section; the dimensions are shown in Fig. 5. The network of finite elements and the kinematic boundary conditions are shown in the same figure.

With increasing loads the stress state in some of elements approaches the failure. At approximately constant volume (ν→0.50) the deviatoric strains tend to increase towards infinity (G→0). In order to avoid the undefiniteness of the stiffness matrix, ν=0.50 has been replaced by 0.499, and G= 0 by G=10^{-10} kp cm^{-2} in the elements where failure stress states had appeared. In this state the elements have been called "plastified" and groups of such elements considered as "plastified zones". In Figs. 5 and 6 the plastified zones have been denoted by the number of the load step when the plastification appeared, the amount of each step being Δq = 0.05 kp cm^{-2}. However, it should be pointed out that in these figures the zones are denoted as plastified even when only in each second finite element the stress state approaches the failure. For this reason the settlements of the layer surface above such zones remain finite until all elements along the width of a continuous zone get plastified.

Plastified zones shown in Fig. 5 have been obtained by taking into account the compression and shear moduli from drained tests (see Figs. 3-b and 4-b). The zones presented in Fig. 6 correspond to undrained conditions (ν=0.50) whereby the shear moduli were assumed to have the same values as in drained conditions. The settlements of the surface corresponding to the 5th, 15th and 25th load step (q=0.25, 0.75 and 1.25 kp cm^{-2} resp.) are presented in Fig. 7. For the 25th increment

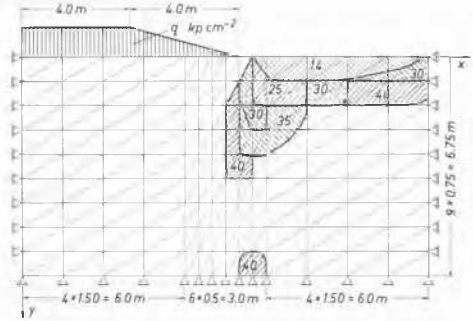

Fig.5 The boundary conditions and the plastified zones according to drained test results for a marsh clay.

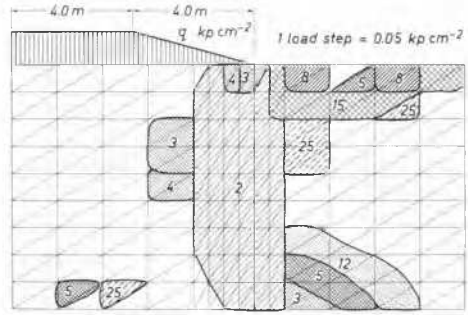

Fig.6 The plastified zones according to undrained test results for a marsh clay.

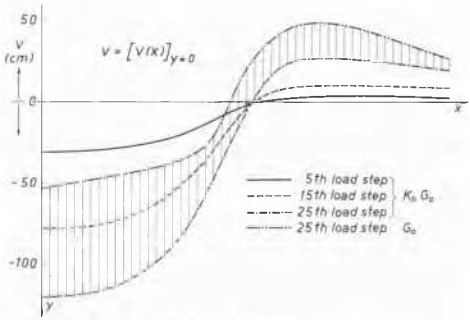

Fig.7 Surface settlements.

the instantaneous ("undrained") settlements are shown as well. Owing to the extremely high compressibility of the marsh clay considered, the amount of settlements is very important. For comparison we note that the total ("drained") settlements would be about

15-times smaller and the instantaneous ("undrained") settlements about 30-times smaller if the layer consisted of the silty sand the deformability of which has been presented in Figs. 1 and 2 (see Battelino 1976).

CONSOLIDATION

In Fig. 8 the development of settlements with time has been shown. The analysis was made in an approximate way by taking for the difference between total and instantaneous settlements at any time the same value of the consolidation degree as for the pure spheric components of settlements. Thereby the spheric components of total stresses were assumed not to be influenced by the consolidation. The increase of the final load up to q=0.75 kp cm^{-2} during six months, and drained upper and lower boundary of the layer were assumed. In Fig. 9 the development of pore pressures with time has been presented for two selected points in the layer. The analysis has been performed by the differential method taking into account the two-dimensional seepage of the pore-water.

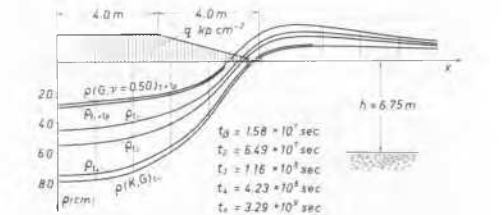

Fig.8 Settlement at times t_i.

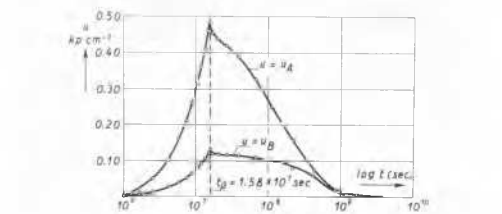

Fig.9 Development of pore pressures in points A(x=1.50m,y=0.75m)and B(x=7.5m,y=0.75m).

CONCLUSIONS

If in triaxial testing of the deformability the stress paths were similar as in the problem to be solved, the treatment of the soil as a "hybrid hypoelastic body" (Desai 1972) seems to be successful. For the use in the finite element analysis the observed stress-strain relationships have been recommended to be transformed into two families of charts relating tangent compression and shear moduli versus octahedral stresses; whatever the shape of charts, they can always be expressed by sets of point values and the interpolation made by using spline functions. The usefulness of the procedure has been proved by applying it for the analysis of settlements and plastification of a very compressible clayey layer subjected to the strip-load by an embankment. The consolidation process has been analyzed in an approximate way by the numerical solution of the differential equation of the two-dimensional consolidation.

ACKNOWLEDGEMENTS

The paper refers to a part of the study on the stress-strain-time relationships for soils which in the years 1975/76 was elaborated in the Soil Mechanics Laboratory at the Civil Engineering Department, University of Ljubljana, under the supervision of Prof. L. Šuklje; the study was financially supported by the Boris Kidrič Fund. The authors wish to express their gratitude to Prof. Šuklje for his assistance in preparing the paper. They acknowledge with thanks the participation of Mr. I. Kovačič who made the program for the two-dimensional consolidation analysis applied in the paper.

REFERENCES

Desai, C.S. (1971), "Nonlinear Analyses Using Spline Functions", Journal of the Soil Mechanics and Foundations Division, ASCE, Vol. 97, No. SM 10, Proc. Paper 8462, Oct. 1971, pp. 1461-1480.

Desai, C.S. (1972), "Theory and Application of the Finite Element Method in Geotechnical Engineering", State-of-the-art: Overview, trends and projections, US Army Eng. Waterways Exp. Station, Corps of Engineers, Vicksburg, Mississippi, pp. 3-90.

Battelino, D. (1976), "Rheological Relationships for Soils according to Experiments and in the Settlement Analysis", Thesis, University of Ljubljana, Civil Engineering Department, 119 p.

Kulhawy, R.M., Duncan, J.M., and Seed, H.B. (1969), "Finite Element Analysis of Stresses and Movements in Embankments during Construction", Report No. Tr 70-20, Office of Research Services, University of California, Berkeley.

Lade, P.V., and Duncan, J.M. (1975), "Elastoplastic Stress-Strain Theory for Cohesionless Soil", Journal of the Geotechnical Engineering Division, ASCE Vol. 101, No. GT 10, Proc. Paper 11670, Oct. 1975, pp. 1037-1053.

Majes, B. (1974), Discussion. Proc. 4th Danube European Conf. Soil Mech. Found. Eng., Bled, II: 68-70.

Prévost, J.H., and Höeg, K. (1975), "Soil Mechanics and Plasticity Analysis of Strain Softening", Geotechnique 25, No. 2, pp. 279-297.

Saje, M. (1974), Discussion. Proc. 4th Danube European Conf. Soil Mech. Found. Eng., Bled, II: 82-83.